International Journal of Earth Sciences Knowledge and Applications
journal homepage: http://www.ijeska.com/index.php/ijeska

Research Article

e-ISSN: 2687-5993

An Experimental Study of the Effect of CO_2 Water-Mancos Shale Interactions on Permeability

James Sheng[1,2]*, Jiahui Zhao[3], Ping Yue[1,3]*

[1]*China University of Petroleum, Beijing, China*
[2]*Texas Tech University, Lubbock, Texas, USA*
[3]*Southwest Petroleum University, Chengdu, China*

INFORMATION

Article history
Received 06 August 2021
Revised 17 August 2021
Accepted 18 August 2021

Keywords
CO_2 water
Mancos Shale
Water-shale interactions
Permeability
Dissolution

Contact
*James Sheng
james.sheng@ttu.edu
*Ping Yue
yuepingaa@126.com

ABSTRACT

When CO_2 water contacts with a split shale rock, it dissolves some mineral components, making the fracture (split) opening wider and the increase in the rock flow capability (apparent permeability) higher. Meanwhile, some dissolved particles move with the flowing water, thus blocking some pore throats and decreasing the rock apparent permeability. Whether the rock apparent permeability can be increased or decreased, depending on these two competitive phenomena. The issue is critical in a carbon capture, utilization, and sequestration project; it is also very important in an enhanced oil recovery project by CO_2 injection. In this study, a split Mancos Shale core was used to investigate this issue. It was found that the apparent permeability was decreased. More research is needed to address this issue.

1. Introduction

When CO_2 is dissolved in water, a carbonic acid solution is formed. Carbonic acid is a kind of weak acid, but its pH value could be low at high pressure. The acidic solution could dissolve calcite and dolomite fast, and quartz and clay slowly. The dissolution reactions may remove some particles. If precipitated particles are not aggregated to block flow channels, the rock permeability should be increased, as some experiments reported (Andreani et al., 2008; Garing et al., 2015; Lu et al., 2016).

Precipitation and clogging depend on many factors, such as cementing minerals, formation water composition, formation temperature, etc. When the formation water is sulfate-rich, gypsum precipitation would be triggered (Dávila et al., 2017). If the cementing minerals are fast-reactive, the slow-reactive minerals will be detached and flow to clog pore throats (Noiriel et al., 2007; Andreani et al., 2008). Noiriel et al. (2007) conducted acidic water flooding experiments. They used fractured argillaceous limestone cores (73% carbonates). Their experiments showed that the porosity was increased due to mineral dissolution. The fracture aperture was increased at some positions, but the average aperture was decreased. The fracture surface roughness was increased due to the removal of dissolvable minerals. The massive displacement of dissolved clays clogged the fracture. The increase in surface roughness and the fracture clogging caused a progressive reduction in permeability. Garing et al. (2015) and Deng et al. (2017) conducted experiments similar to Noiriel et al. (2007) and obtained similar results, except that Deng et al. (2017) did not observe clogging.

Tutolo et al. (2015) conducted CO_2-charged brine flooding experiments. The rock core used was Eau Claire feldspar-rich

arkose sandstone, 12.8 mm in diameter and 24.9 mm in length without being fractured. The results show that the core bulk permeability (initially about 50 mD) decreased during the experiment. K-feldspar was reacted and dissolved, and aluminum minerals were precipitated. Due to CO_2-acidified fluid etching of grain surfaces, the porosity was increased. But the permeability was decreased due to the production and precipitation of secondary Al-rich minerals, including the generation of kaolinite. Precipitation occurred in preferential flow channels in the core, which caused a decrease of porosity in those certain sections, but the porosity of the entire core was increased. The decrease of porosity in preferential flow channels decreased the permeability, even though the porosity is increased in other slow flow areas.

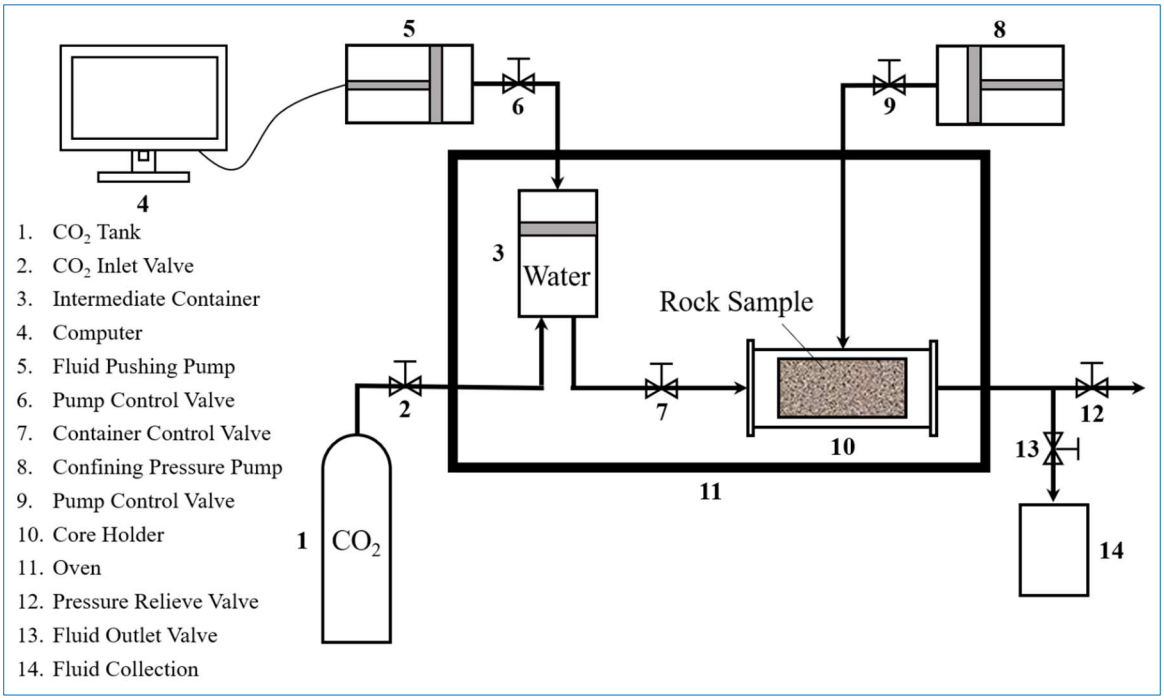

Fig. 1. Schematic of the experimental setup

Deng et al. (2018) did a simulation related to flow rate patterns. The simulated rock was based on Eagle Ford and Niobrara Shales (> 30% calcite) with 25.4 mm in width and 50.8 in length. Three flow rate patterns were simulated: 0.01, 0.1, and 1 mL/min. The simulation result shows distinct dissolution regimes at different flow rates, each regime produces a characteristic dissolution pattern of chemical reactions and fracture hydraulic properties. As flow rate increases, fracture evolution shifts from compact dissolution to fracture channelization to uniform dissolution. In the case of compact dissolution, fracture permeability does not increase significantly because of the lack of fracture opening at the downstream end. At a flow rate that is slow compared to the reaction rate, the residence time of the fluid is much longer than the time of reactions, local equilibrium is likely to be achieved.

Table 1. Mineralogical composition of Mancos Shale

The proportion of minerals in shale (%)							
Quartz	**Potassium feldspar**	**Plagioclase**	**Calcite**	**Ankerite**	**Siderite**	**Pyrite**	**Total clay**
55	3	5	8	12	1	1	15
The proportion of clay minerals in total clay (%)							
Illite		**Kaolinite**		**Chlorite**		**Mixed layer (illite/montmorillonite)**	
30		7		2		61	
The proportion of layers in mixed-layer clay (%)							
Montmorillonite					**Illite**		
30					70		

As a result, reactions and the resulting aperture change are limited to the inlet of the flow. In the case of uniform dissolution, fracture permeability will increase substantially when no confining stress is present and can decrease under confining stresses because of the removal of contact points. At a flow rate that is faster than the reaction rate, the residence time of the fluid is short, and local reactions become surface reaction controlled.

Consequently, highly reactive fluids persist throughout the length of the fracture, and dissolution is uniform in the fracture. Fracture channelization leads to a rapid increase in fracture permeability, even under confining pressure, as contact points in non-channelized regions in the fracture are preserved and can prevent the fracture from closing. At flow rates that are comparable to the reaction rate, the interplay between flow and reactions leads to reactive infiltration instability, the perturbations due to geometric, flow, and geochemical heterogeneity are amplified to create preferential flow channels in the fractures.

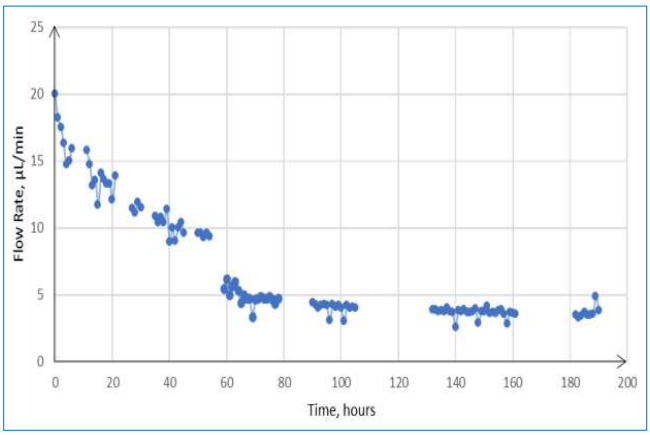

Fig. 2. Flow rate history for CO_2 water experiment

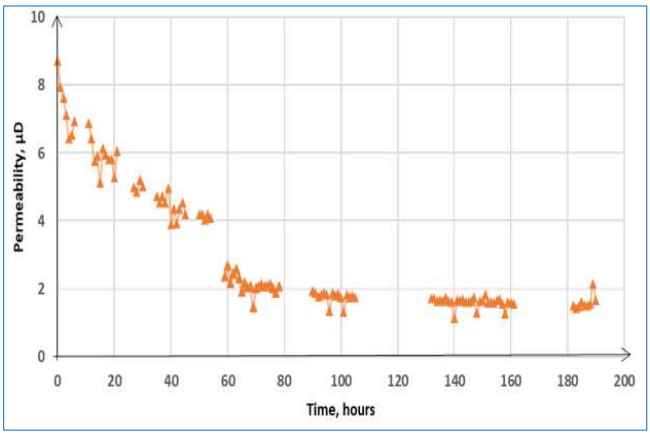

Fig. 3. Apparent permeability change during CO_2 water experiment

Most of the studies as referred to above dealt with CO_2-rich solutions. Even dry supercritical CO_2 can react with calcite and dolomite, but it can only etch calcite surfaces (Lu et al., 2016; Sanguinito et al., 2018). It can also cause pyrite oxidation (Lu et al., 2016). It may also cause precipitation which will decrease permeability.

Luquot et al. (2016) conducted similar experiments using Heletz sandstone with 10-40 mD. But they observed that the permeability was increased because precipitated particles flowed out of the cores. CO_2 injection will affect (shale) rock properties. Generally, CO_2 injection will make shale rock less hydrophilic, weaken shale rock mechanical strength and increase shale ductility (Fatah et al., 2020).

This paper is to conduct flooding experiments to see how the permeability of a core with an existing fracture and the fracture itself change when CO_2 water is flowing through the fracture.

2. Experimental Setup

The schematic of the experimental setup is shown in Fig. 1. CO_2 from CO_2 tank 1 and water from pump 5 were mixed in the intermediate container 3 to form a CO_2 water solution. The solution flowed through core 10. The pressures at the core inlet and outlet and the flow rate through pump 5 were recorded.

The core used was a 3-in Mancos Shale sample. The shale sample was split along its cylindrical axis by using the Brazilian test method. The length L was 69.5 mm (0.0695 m), the diameter D was 37.5 mm (0.0375 m), and the cross-sectional area A was 1104 mm2 (0.001104 m2). The temperature was set at 40 ºC, and the viscosity of water used in the experiment at 40 ºC was 0.7 mPa·s (0.0007 Pa·s).

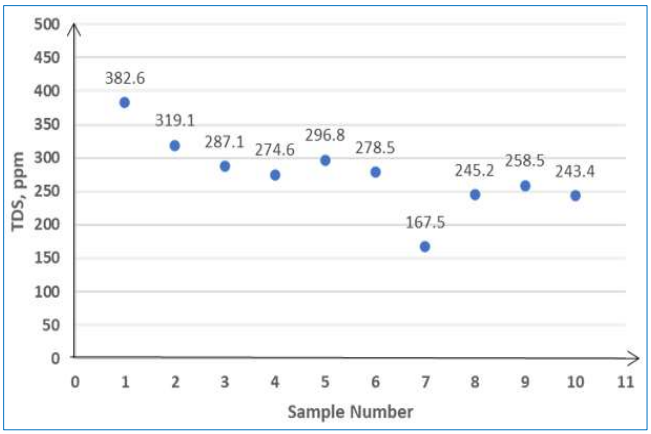

Fig. 4. Salinity (total dissolved solid: TDS) changes of outlet fluid samples

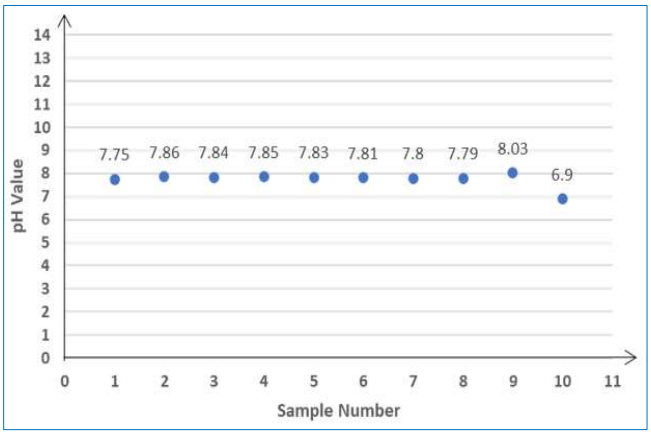

Fig. 5. pH changes of outlet fluid samples

The Mancos Shale core was an outcrop core. The mineralogical composition of the shale sample was determined by X-ray diffractometry. As shown in Table 1, quartz was dominant and the total clay proportion was 15%. Illite and mixed-layer clay were the main types of clays. The

illite content was 30%, and the mixed-layer clay content was 61% with a little kaolinite and chlorite. The changes of fracture aperture and fracture surfaces were investigated using naked eyes. The apparent core permeability changes during the flow were calculated according to Darcy's equation.

3. Results and Discussion

In a CO_2 water experiment, the confining pressure pc was 1300 psi, the backpressure pb was 725 psi, the inlet pressure pin is 975 psi, and thus the inlet-outlet pressure difference Δp was 250 psi. The flow rate history and apparent permeability changes are shown in Figs. 2 and 3, respectively.

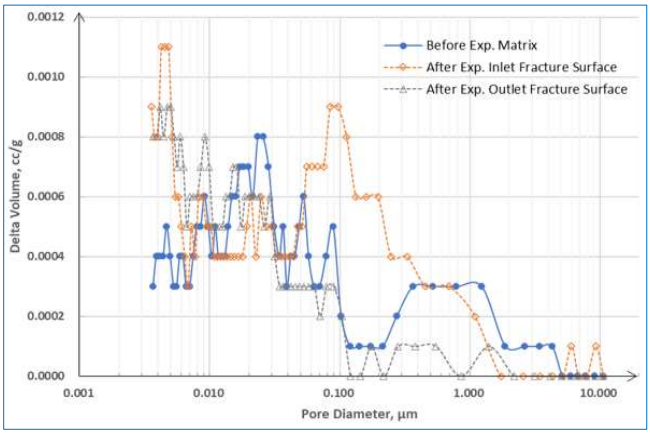

Fig. 6. Comparison of pore size distribution before and after the experiment

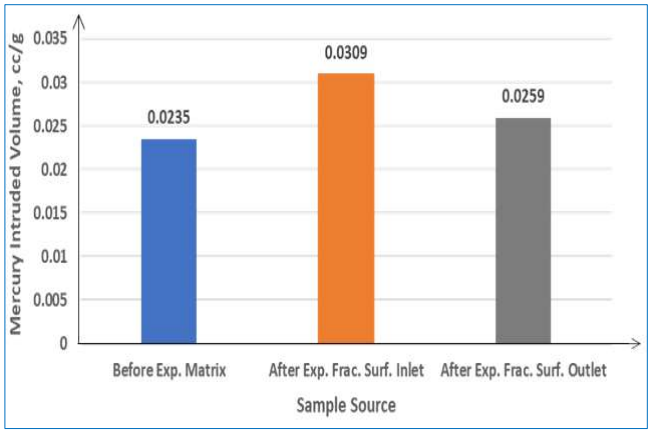

Fig. 7. Comparison of Mercury Intruded Volume

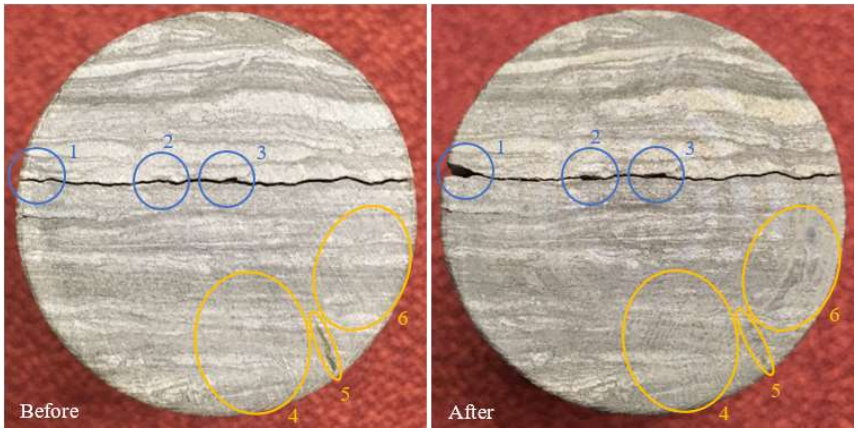

Fig. 8. Comparison of the inlet side surface of the Mancos Shale sample before and after the experiment

The apparent permeability was calculated using Darcy's equation. The gaps in the curves are caused by missing data when outlet fluid samples were collected. During this time, we were busy collecting data, and flow rate data were not recorded. Fig. 3 shows that the apparent permeability was decreasing during the experiment

The salinity and pH values of outlet fluid samples were measured by Thermo Scientific Orion Star A215 pH/Conductivity Meter. Their changes during the experiment are shown in Figs. 4 and 5. The salinity slightly decreased, and the pH hardly changed, indicating the consumption reaction was not significant.

The pore size distribution was measured using Quantachrome PoreMaster automatic pore size analyzer. Before the experiment, a rock matrix sample was collected to measure the initial pore size distribution. After the experiment, two samples were collected from the fracture surface. One from the inlet side and the other one from the outlet side were used to measure the pore size changes. The pore size distributions and mercury intruded volumes are summarized in Figs. 6 and 7, respectively. It is shown that the pore size was increased at the inlet side and decreased at the outlet side. Moreover, the near-fracture pore volume at the inlet side was increased, whereas the near-fracture pore volume at the outlet side did not change too much. The result indicates that the porosity in the near-fracture area was increased, and reaction and dissolution mainly occur at the inlet side of the fracture.

The surface structures of the shale sample before and after the experiment are shown in Fig. 8. The fracture aperture was increased at some positions after the experiment as indicated with blue circles 1, 2, and 3 in Fig. 8. Some obvious precipitations were also observed on the surface of the sample as indicated with orange ellipses 4 and 6 in Fig. 8. In orange ellipse 5, mineral with dark color was reacted and dissolved.

The increase of fracture aperture was also observed on the cylindrical side of the shale sample as indicated with orange ellipse 7 in Fig. 9. On the fracture surface, reaction and dissolution were observed due to the disappearance of some white minerals (calcite or dolomite, as indicated with orange circles 8, 9, and 10 in Fig. 10).

Fig. 9. Comparison of the cylindrical side surface of Mancos Shale sample

Fig. 10. Comparison of the fracture surface of Mancos Shale sample

4. Concluding Remarks

When CO_2 water contacts with a split shale rock, it dissolves some mineral components, making the fracture opening wider and resulting in the increase in the rock flow capability (apparent permeability calculated using Darcy's equation) higher. Meanwhile, some dissolved particles move with the flowing water, thus blocking some pore throats and decreasing the rock apparent permeability. Whether the rock apparent permeability can be increased or decreased, depending on the two competitive phenomena. It was found in this experiment that the apparent permeability was decreased. More research is needed to answer the question.

Data Availability Statement

Some or all data, models, or codes that support the findings of this study are available from the corresponding author upon reasonable request.

Acknowledgments

The work presented in this paper is supported by the Fundamental Research Funds for the Central Universities of China and the Strategic Cooperation Technology Projects of CNPC and CUPB (ZLZX2020).

References

Andreani, M., Gouze, P., Luquot, L., Jouanna, P., 2008. Changes

in seal capacity of fractured claystone caprocks induced by dissolved and gaseous CO_2 seepage. Geophysical Research Letters 35, L14404.

Dávila, G., Cama, J., Luquot, L., Soler, J. M., Ayora, C., 2017. Experimental and modeling study of the interaction between a crushed marl caprock and CO_2-rich solutions under different pressure and temperature conditions. Chemical Geology 448, 26-42.

Deng, H., Steefel, C., Molins, S., DePaolo, D., 2018. Fracture evolution in multimineral systems: The role of mineral composition, flow rate, and fracture aperture heterogeneity. ACS Earth and Space Chemistry 2 (2), 112-124.

Deng, H., Voltolini, M., Molins, S., Steefel, C., DePaolo, D., Ajo-Franklin, J., Yang, L., 2017. Alteration and erosion of rock matrix bordering a carbonate-rich shale fracture. Environmental Science & Technology 51 (15), 8861-8868.

Fatah, A., Bennour, Z., Mahmud, H.B., Gholami, R., Hossain, M.M., 2020. A Review on the Influence of CO_2/Shale Interaction on Shale Properties: Implications of CCS in Shales. Energies 13 (12), 3200.

Garing, C., Gouze, P., Kassab, M., Riva, M., Guadagnini, A., 2015. Anti-correlated porosity–permeability changes during the dissolution of carbonate rocks: experimental evidences and modeling. Transport in Porous Media 107 (2), 595-621.

Lu, J., Nicot, J.P., Mickler, P. J., Ribeiro, L.H., Darvari, R., 2016. Alteration of Bakken reservoir rock during CO_2-based fracturing - An autoclave reaction experiment. Journal of Unconventional Oil and Gas Resources 14, 72-85.

Luquot, L., Gouze, P., Niemi, A., Bensabat, J., Carrera, J., 2016. CO_2-rich brine percolation experiments through Heletz reservoir rock samples (Israel): Role of the flow rate and brine composition. International Journal of Greenhouse Gas Control 48, 44-58.

Noiriel, C., Madé, B., Gouze, P., 2007. Impact of coating development on the hydraulic and transport properties in argillaceous limestone fracture. Water Resources Research 43, W09406.

Sanguinito, S., Goodman, A., Tkach, M., Kutchko, B., Culp, J., Natesakhawat, S., Fazio, J., Fukai, I., Crandall, D., 2018. Quantifying dry supercritical CO_2-induced changes of the Utica Shale. Fuel 226, 54-64.

Tutolo, B.M., Luhmann, A.J., Kong, X.Z., Saar, M.O., Seyfried, W.E., 2015. CO_2 sequestration in feldspar-rich sandstone: coupled evolution of fluid chemistry, mineral reaction rates, and hydrogeochemical properties. Geochimica et Cosmochimica Acta 160, 132-154.